ansa-Metallocene Derivatives. 24. Deviations from C_2-Axial Symmetry in Ethano- and Etheno-Bridged Titanocene Complexes: Investigation of *ansa*-Metallocene Conformations[1]

Peter Burger, Josef Diebold, Stephan Gutmann, Hans-Ulrich Hund, and Hans-Herbert Brintzinger*

Fakultät für Chemie, Universität Konstanz, D-7750 Konstanz, FRG

Received July 17, 1991

One ethano- and two etheno-bridged titanocene dichloride complexes without further substituents at their cyclopentadienyl ring ligands are found to crystallize with molecular structures which deviate substantially from the expected C_2-axial symmetry. X-ray diffraction studies give space group $P2_12_12_1$ with a = 771.9 (1) pm, b = 1785.3 (4) pm, and c = 1883.6 (3) pm (Z = 8) for the dimethyletheno-bridged complex $C_2(CH_3)_2[1\text{-}C_5H_4]_2TiCl_2$, space group $P2_1/c$ with a = 867.7 (4) pm, b = 1611.3 (7) pm, c = 1377.6 (7) pm, and β = 91.48 (4)° (Z = 4) for the diphenyl analogue $C_2(C_6H_5)_2[1\text{-}C_5H_4]_2TiCl_2$, and space group $P\bar{1}$ with a = 1072.8 (2) pm, b = 1266.0 (3) pm, c = 1511.0 (3) pm, α = 80.66 (3)°, β = 89.04 (3)°, and, γ = 76.20 (3)° (Z = 4) for the bis(pentamethylene)ethano-bridged titanocene complex $C_2((CH_2)_5)_2[1\text{-}C_5H_4]_2TiCl_2$. Space group $P2_1/c$ with a = 959.4 (3) pm, b = 1284.2 (3) pm, c = 2379.9 (7) pm, and β = 111.73 (2)° (Z = 4) is found for the tetramethylethano-bridged, bis(dimethylfurfuryl)-substituted titanocene derivative *rac*-$C_2(CH_3)_4[1\text{-}C_5H_3\text{-}3\text{-}C(CH_3)_2(2'\text{-}C_4H_3O)]_2TiCl_2$. Analysis of nonbonding contacts in these complexes reveals that *intra*molecular repulsions between Cl ligand atoms and β-H and -C atoms of each ring ligand induce a rotation of the bridged ligand framework about the metal–C_5-ring-centroid axes toward one of two shallow energy minima which are located about ±20° away from the $TiCl_2$ bisector axis. In solution, NMR spectra indicate unrestricted fluctuation between these two conformations. Effects of α- or β-alkyl substituents at the C_5 rings and of different bridging units and coligands on the relative stability of axially symmetric and off-axially distorted conformers are analyzed with regard to chiral *ansa*-metallocenes used in homogeneous Ziegler–Natta catalysis.

Introduction

Chiral metallocene derivatives of group 4 transition metals, in which both cyclopentadienyl ligands are substituted in an axially symmetric manner and, in addition, connected by an interannular ethano or silano bridge, show interesting properties as α-olefin polymerization catalysts when activated by methylalumoxane or by other agents capable of generating reactive alkyl cations.[2] The rather high stereoselectivity for isotactic olefin insertion frequently observed for these catalysts is thought to be connected with the stereorigidity of their ligand framework, in which the short interannular bridge maintains a C_2-symmetrical geometry with two equivalent coordination sites of identical chiral environment.[3]

While C_2-axial symmetry has been observed, by X-ray structure determinations, for quite a number of chiral *ansa*-metallocene derivatives,[4-9] a few cases have recently been encountered[7,9] in which a ligand framework carrying two bulky alkyl substituents—although axially symmetric in itself—is out of axial alignment with the $TiCl_2$ moiety by 30° or more (Figure 1). These observations have raised the possibility that bulky substituents at the C_5-ring ligands might cause such deviations from C_2-axial symmetry.

Here, we report on several cases where similar distortions occur in *ansa*-titanocene derivatives with ethano- or etheno-bridged, but otherwise unsubstituted, cyclopentadienyl ligands (cf. Chart I). This observation has led us to investigate the factors which determine the conformational geometry of *ansa*-metallocene complexes.

Chart I

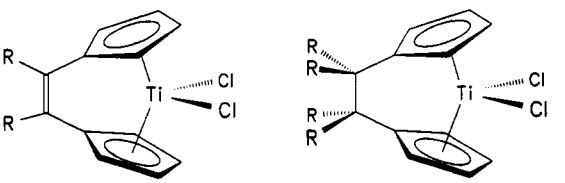

2 R : $-CH_3$ 4 R , R : $-(CH_2)_5-$

3 R : $-C_6H_5$ 5 R , R : −H , −H

Results and Discussion

Crystal structures of the two etheno-bridged titanocene complexes **2** (R = CH_3) and **3** (R = C_6H_5),[11] as determined

(1) Part 23: Burger, P.; Hortmann, K.; Diebold, J.; Brintzinger, H. H. *J. Organomet. Chem.* **1991**, *417*, 9.

(2) For recent reviews of this topic see, e.g.: (a) Jordan, R. F.; Bradley, P. K.; LaPointe, R. E.; Taylor, D. F. *New J. Chem.* **1990**, *14*, 505. (b) Spaleck, W.; Antberg, M.; Dolle, V.; Klein, R.; Rohrmann, J.; Winter, A. *New J. Chem.* **1990**, *14*, 499. (c) Antberg, M.; Dolle, V.; Haftka, S.; Rohrmann, J.; Spaleck, W.; Winter, A.; Zimmerman, H. J. Proceedings of the 3rd European Polymer Federation Symposium. *Makromol. Chem., Macromol. Symp.* **1991**, *48/49*, 333. (d) Ewen, J. A.; Elder, M. J.; Jones, R. L.; Haspeslagh, L.; Atwood, J. L.; Bott, S. G.; Robinson, K. Proceedings of the 3rd European Polymer Federation Symposium. *Makromol. Chem., Macromol. Symp.* **1991**, *48/49*, 253.

(3) Olefin polymerization by unbridged, chiral zirconocene derivatives is partially stereoselective at ca. −80 °C: Erker, G.; Nolte, R.; Tsay, Y. H.; Krüger, C. *Angew. Chem.* **1989**, *101*, 642.

(4) (a) Smith, J. A.; von Seyerl, J.; Huttner, G.; Brintzinger, H. H. *J. Organomet. Chem.* **1979**, *173*, 175. (b) Wochner, F.; Zsolnai, L.; Huttner, G.; Brintzinger, H. H. *J. Organomet. Chem.* **1985**, *288*, 69.

(5) Wild, F. R. W. P.; Zsolnai, L.; Huttner, G.; Brintzinger, H. H. *J. Organomet. Chem.* **1982**, *232*, 233. Wild, F. R. W. P.; Wasiucionek, M.; Huttner, G.; Brintzinger, H. H. *J. Organomet. Chem.* **1985**, *288*, 63. Ewen, J. A.; Haspeslagh, L.; Atwood, J. L.; Zhang, H. *J. Am. Chem. Soc.* **1987**, *109*, 6544. Collins, S.; Kuntz, B. A.; Taylor, N. J.; Ward, D. G. *J. Organomet. Chem.* **1988**, *342*, 21.

(6) Herrmann, W. A.; Rohrmann, J.; Herdtweck, E.; Spaleck, W.; Winter, A. *Angew. Chem.* **1989**, *101*, 1536.

(7) (a) Gutmann, S.; Burger, P.; Hund, H. U.; Hofmann, J.; Brintzinger, H. H. *J. Organomet. Chem.* **1989**, *369*, 343. (b) Gutmann, S. Dissertation, Konstanz, FRG, 1989. (c) Burger, P. Dissertation, Konstanz, FRG, 1991.

(8) Wiesenfeldt, H.; Reinmuth, A.; Barsties, E.; Evertz, K.; Brintzinger, H. H. *J. Organomet. Chem.* **1989**, *369*, 359.

(9) Collins, S.; Hong, Y.; Taylor, N. J. *Organometallics* **1990**, *9*, 2695. These authors report the occurrence of axially symmetric and nonaxially distorted forms in different crystal modifications of the same compound, *rac*-$C_2H_4(1\text{-}C_5H_3\text{-}3\text{-}C(CH_3)_3)_2TiCl_2$.

0276-7333/92/2311-1319$03.00/0

Table I. Bonding and Nonbonding Distances (in pm) and Bond and Dihedral Angles (in deg) with Esd's in Parentheses for Complex 1, *rac*-$C_2(CH_3)_4[1\text{-}C_5H_3\text{-}3\text{-}C(CH_3)_2(2'\text{-}C_4H_3O)]_2TiCl_2$[a]

	Distances and Angles		
Ti(1)–Cl(1)	232.7 (2)	Ti(1)–CR(1)	208.1
Ti(1)–Cl(2)	238.4 (2)	Ti(1)–CR(2)	208.3
Ti(1)–C(1)	232.8 (5)		
Ti(1)–C(2)	240.9 (4)	Cl(1)–Ti(1)–Cl(2)	95.7 (1)
Ti(1)–C(3)	250.8 (4)	CR(1)–Ti(1)–CR(2)	128.2
Ti(1)–C(4)	243.5 (4)	PL(1)–PL(2)	59.4
Ti(1)–C(5)	234.2 (4)		
Ti(1)–C(19)	236.2 (4)	CR(1)–C(1)–C(13)	1.3 (exo)
Ti(1)–C(20)	238.0 (4)	CR(2)–C(19)–C(16)	3.2 (exo)
Ti(1)–C(21)	250.4 (4)	CR(1)–C(3)–C(6)	8.6 (exo)
Ti(1)–C(22)	242.0 (4)	CR(2)–C(21)–C(24)	11.2 (exo)
Ti(1)–C(23)	235.6 (4)		
C(13)–C(16)	161.1 (5)	C(1)–C(13)–C(16)–C(19)	33.8 (4)
ZCP-ZZ-ZCL	143.6		
	Intramolecular Contacts		
Cl(2)···H(2)	297	Cl(2)···H(23)	296
Cl(2)···C(23)	298		

[a] Legend: CR = centroid; PL = mean plane of η^5-C_5 ring; ZCP = midpoint of the vector connecting the two bridgehead carbon atoms C(1) and C(19), ZCL = midpoint of the Cl–Cl vector, ZZ = midpoint of the CR–CR vector.

by X-ray diffraction (see Experimental Section), are represented in Figure 2, while Figure 3 shows the structure of the bis(pentamethylene)ethano-bridged complex **4** (R, R = $-(CH_2)_5-$)[10] and, for comparison, the previously reported axially symmetric structure of **5** (R, R = –H, –H).[4a] The interannular bridges of complexes **2–4** are all distinctly misaligned relative to their $TiCl_2$ fragments. In each case, the $TiCl_2$ bisector axis deviates by ca. 20° from the axis which connects the Ti center with the midpoint of the C_2 bridge.

With respect to their coordination geometry parameters, i.e. Ti–C and Ti–Cl bond lengths as well as Cl–Ti–Cl and centroid–Ti–centroid angles (Tables II–IV), complexes **2–4** are entirely within the range normally found for other titanocene dichloride species.[4-9,12] The distorted structures of **2–4** are best described as arising from a rotation of the C_5-ring ligands about the respective metal–centroid axes, away from an idealized C_{2v}-symmetric geometry, by some specified torsional angle θ. Consymmetric[13] rotation of both rings with $\theta \approx \pm 20°$ produces the geometry found for the etheno-bridged complexes **2** and **3**. For the two rings of complex **4**, we find $\theta = +26°$ and $-12°$, i.e. $|\theta| = 19 \pm 7°$, relative to an assumed C_{2v}-symmetric geometry. In comparison to the C_2-symmetric structure of complex **5**, however, which itself deviates from C_{2v} symmetry by a dissymmetric[13] rotation of both rings with $\theta \approx +6°$, the geometry of **4** corresponds, again, to a consymmetric rotation of the ligand framework with $\theta \approx \pm 20°$.

(10) Compounds **1** and **4** were prepared, via Mg/CCl_4-induced reductive coupling of 2-(α,α-dimethyl-2-furfuryl)-6,6-dimethylfulvene[7b] and of 6,6-pentamethylenefulvene (Stone, K. J.; Little, R. D. *J. Org. Chem.* **1984**, *49*, 1849), respectively, by the procedure described for $(CH_3)_4C_2(C_5H_4)_2TiCl_2$ (Schwemlein, H.; Brintzinger, H. H. *J. Organomet. Chem.* **1983**, *254*, 69). ^1H NMR data for *rac*-**1** (C_6D_6 solution; δ in ppm): 6.97 (d), 6.67 (d), 6.34 (p), 6.13 (p), 5.97 (d), 5.81 (d), 2.00 (s), 1.95 (s), 0.94 (s), 0.86 (s) (d = doublet of doublets, 2 H; p = pseudotriplet, 2 H; s = singlet, 6 H).

(11) Preparation of complexes **2** and **3**: Burger, P.; Brintzinger, H. H. *J. Organomet. Chem.* **1991**, *407*, 207.

(12) See: Orpen, A. G.; Brammer, L.; Allen, F. H.; Kennard, O.; Watson, D. G.; Taylor, R. *J. Chem. Soc., Dalton Trans.* **1989**, S1 and literature cited therein.

(13) Rotation of both rings about the respective metal–centroid axes with identical, positive torsional angles θ generates a dissymmetric, racemic conformer as in **5**; C_s-symmetric meso conformers as in **2** and **3** arise by a rotation of both rings with torsional angles of opposite sign. This torsional mode is henceforth termed "consymmetric".

Table II. Bonding and Nonbonding Distances (in pm) and Bond and Dihedral Angles (in deg) with Esd's in Parentheses for Complex 2, $C_2(CH_3)_2[1\text{-}C_5H_4]_2TiCl_2$[a]

	Distances and Angles		
Ti(1)–Cl(1)	236.6 (1)	Ti(2)–Cl(3)	235.8 (1)
Ti(1)–Cl(2)	235.1 (1)	Ti(2)–Cl(4)	235.8 (1)
Ti(1)–C(1)	236.1 (4)	Ti(2)–C(15)	234.2 (4)
Ti(1)–C(2)	239.5 (5)	Ti(2)–C(16)	239.4 (5)
Ti(1)–C(3)	238.8 (5)	Ti(2)–C(17)	240.2 (4)
Ti(1)–C(4)	237.0 (4)	Ti(2)–C(18)	239.1 (4)
Ti(1)–C(5)	238.0 (4)	Ti(2)–C(19)	236.9 (4)
Ti(1)–C(10)	237.4 (4)	Ti(2)–C(24)	239.0 (4)
Ti(1)–C(11)	235.9 (5)	Ti(2)–C(25)	236.4 (5)
Ti(1)–C(12)	240.6 (5)	Ti(2)–C(26)	239.9 (5)
Ti(1)–C(13)	239.6 (5)	Ti(2)–C(27)	241.8 (5)
Ti(1)–C(14)	237.5 (4)	Ti(2)–C(28)	238.2 (4)
C(6)–C(8)	132.4 (6)	C(20)–C(22)	132.9 (6)
Ti(1)–CR(1)	205.9	Ti(2)–CR(3)	205.1
Ti(1)–CR(2)	205.6	Ti(2)–CR(4)	207.4
Cl(1)–Ti(1)–Cl(2)	95.5 (1)	Cl(3)–Ti(2)–Cl(4)	93.9 (1)
CR(1)–Ti(1)–CR(2)	128.1	CR(3)–Ti(2)–CR(4)	128.1
PL(1)–PL(2)	53.6	PL(3)–PL(4)	54.3
PL(1)–PLO(1)	81.0	PL(3)–PLO(2)	102.4
PL(2)–PLO(1)	96.4	PL(4)–PLO(2)	84.6
PLO(1)–PLZ(1)	17.8	PLO(2)–PLZ(2)	20.1
C(5)–C(6)–C(8)	117.4 (4)	C(19)–C(20)–C(21)	117.6 (4)
C(21)–C(20)–C(22)	125.0 (4)		
C(9)–C(8)–C(10)	116.5 (4)	C(23)–C(22)–C(24)	117.5 (4)
C(6)–C(8)–C(9)	127.0 (4)	C(20)–C(22)–C(23)	126.6 (4)
C(5)–C(6)–C(8)–C(10)	–1.8 (6)	C(19)–C(20)–C(22)–C(24)	3.7 (6)
C(7)–C(6)–C(8)–C(9)	–2.2 (7)	C(21)–C(20)–C(22)–C(23)	3.1 (8)
	Intramolecular Contacts		
Cl(2)···H(2)	287	Cl(2)···H(12)	287
Cl(1)···C(3)	307	Cl(1)···C(4)	310
Cl(1)···C(13)	309	Cl(1)···C(14)	311
Cl(2)···C(2)	301	Cl(2)···C(12)	299
Cl(3)···H(16)	287	Cl(3)···H(27)	290
Cl(3)···C(16)	301	Cl(3)···C(27)	303
Cl(4)···C(17)	301	Cl(4)···C(18)	312
Cl(4)···C(25)	313	Cl(4)···C(26)	308

[a] Legend: CR = centroid; PL = mean plane of η^5-C_5 ring; PLO = mean plane of olefin π-system; PLZ = plane spanned by centroids and the titanium atom.

Table III. Bonding and Nonbonding Distances (in pm) and Bond and Dihedral Angles (in deg) with Esd's in Parentheses for Complex 3, $C_2(C_6H_5)_2[1\text{-}C_5H_4]_2TiCl_2$[a]

	Distances and Angles		
Ti(1)–Cl(1)	233.1 (5)	Ti(1)–Cl(2)	234.5 (3)
Ti(1)–C(1)	236.8 (10)	Ti(1)–C(2)	237.8 (14)
Ti(1)–C(3)	242.4 (18)	Ti(1)–C(4)	241.3 (14)
Ti(1)–C(5)	234.8 (11)	Ti(1)–C(6)	240.6 (16)
Ti(1)–C(7)	233.8 (14)	Ti(1)–C(8)	238.6 (19)
Ti(1)–C(9)	241.5 (19)	Ti(1)–C(10)	243.5 (19)
C(11)–C(18)	128.1 (22)		
Ti(1)–CR(1)	206.0	Ti(1)–CR(2)	207.4
Cl(1)–Ti(1)–Cl(2)	95.1 (1)	CR(1)–Ti(1)–CR(2)	128.1
PL(1)–PL(2)	53.7		
PL(1)–PLO	74.7	PL(2)–PLO	90.1
PLO–PLZ	22.7		
C(6)–C(18)–C(19)	112.0 (12)	C(11)–C(18)–C(6)	120.5 (13)
C(12)–C(11)–C(1)	116.9 (13)	C(18)–C(11)–C(1)	115.7 (9)
C(1)–C(11)–C(18)–C(6)	8.2 (15)		
	Intramolecular Contacts		
Cl(2)···H(4)	288	Cl(2)···H(9)	287

[a] Legend: CR = centroid; PL = mean plane of η^5-C_5 ring; PLO = mean plane of olefin π-system; PLZ = plane spanned by centroids and the titanium atom.

Crystal-packing effects would appear to be the most likely cause for these distortions. Indeed, one can discern a number of nonsymmetric, intermolecular contacts below the van der Waals limit in the crystal structures of **3** and **4** (cf. Figure 7). For **2**, however, we cannot detect any such

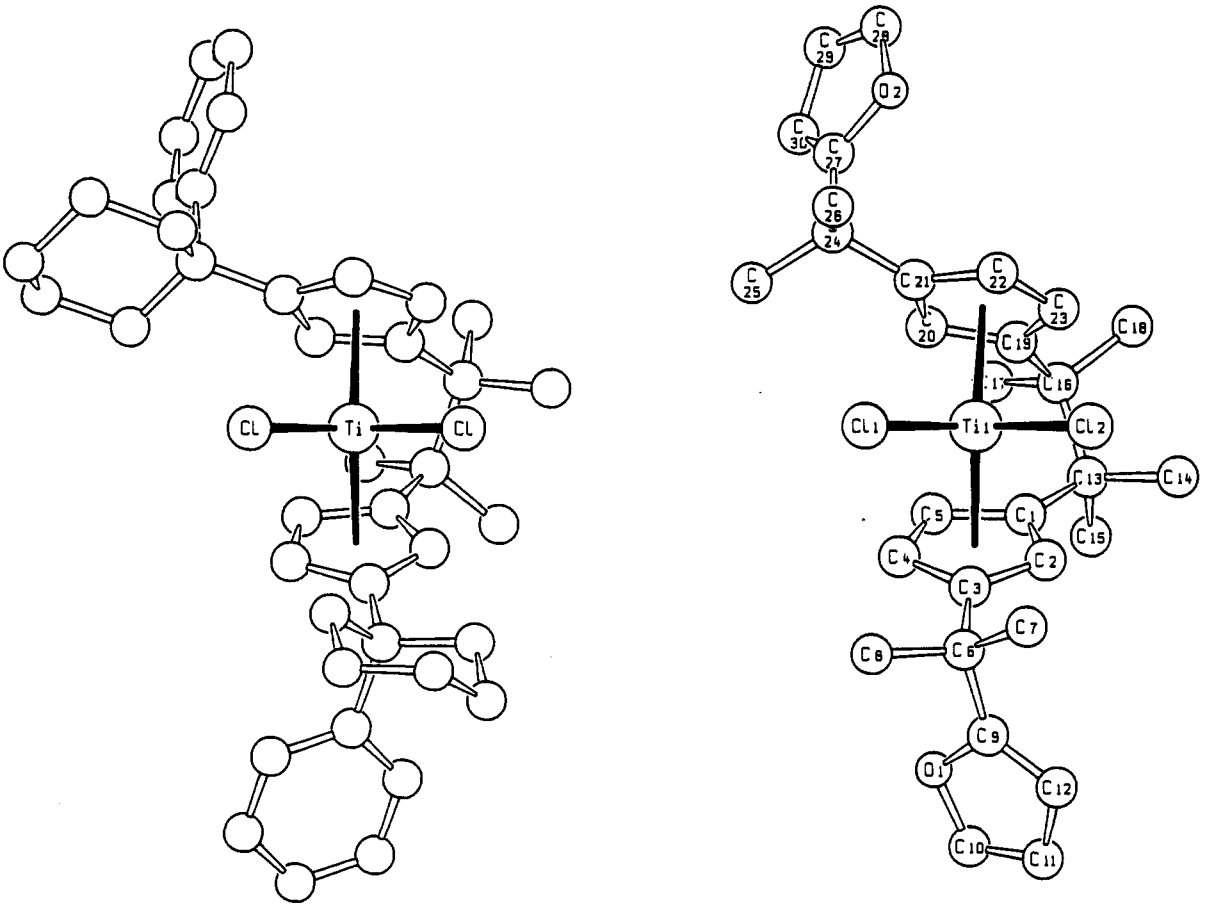

Figure 1. Deviations from axial symmetry observed for the tetramethylethano-bridged, 1'-phenylcyclohexyl-substituted complex $C_2(CH_3)_4[1\text{-}C_5H_3\text{-}3\text{-}C(CH_2)_5(C_6H_5)]_2TiCl_2$ (left, as reported in ref 7a,c), and for the α,α-dimethylfurfuryl-substituted complex 1, $C_2(CH_3)_4[1\text{-}C_5H_3\text{-}3\text{-}C(CH_3)_2(2'\text{-}C_4H_3O)]_2TiCl_2$ (right[10]). Projections are parallel to the $TiCl_2$ bisector axis.

intermolecular contacts with nonbonding distances less than the sum of the van der Waals radii. At least in this case—and by implication also in the others—additional factors must be operative to stabilize the distorted geometries observed for these complexes.

From Figure 4 it is apparent that a number of *intramolecular*, nonbonding contacts below the van der Waals limit occur in complex **2**: In both crystallographically independent molecules, one of the Cl atoms is in repulsive contact with one β-C and one β-H atom, while the other Cl atom is in close contact with one α- and one β-C atom. Following the assumption that these intramolecular distances are decisive for the preferred conformation of these complexes, we have determined, by a model simulation,[14] the nonbonding contact distances between each Cl ligand atom and its α- and β-H and α- and β-C atom neighbors in dependence on the torsional angle θ. The results of this analysis (Figure 5) indicate that for a C_{2v}-symmetric geometry (for $\theta = 0°$) a ring ligand will have both of its β-H and -C atoms close to a Cl atom, at distances below the van der Waals threshold. Rotation of the ring ligand to values of $\theta \approx 20°$ will substantially increase these distances to one set of H and C atoms, while only marginally decreasing distances to the other set: At $\theta \approx 20°$ only one β-H atom at each C_5 ring is in repulsive contact with each Cl atom. Rotation by larger angles would tend to nullify this effect, since another set of C and H atoms would be brought into closer contact with each of the Cl atoms.

In order to estimate the energy changes associated with these intramolecular Cl–H and Cl–C contacts, we consider a model complex of the type $(X\text{-}C_5H_4)_2TiCl_2$ with eclipsed C_5 rings (i.e. with an initial, idealized C_{2v}-symmetric geometry) in which a nonrepulsive dummy atom X (i.e. a void) is attached to both bridgehead atoms C_X instead of the etheno bridge. When the conformational energy profile for this model is calculated by means of a Buckingham-type potential function, we obtain, in agreement with the discussion concerning Figure 5, an energy maximum at $\theta = 0°$ and two energy minima at $\theta \approx \pm 20°$ (Figure 6). While our model would predict, in its simplest form, similar energy gains for consymmetric as well as for dissymmetric rotation of the C_5 rings by $\theta \approx 20°$, only a consymmetric rotation of both rings is compatible with the planarity of an etheno bridge. Such a consymmetric rotation is indeed observed, as discussed above, for the etheno-bridged complexes **2** and **3** (cf. Figure 2).[16]

In ethano-bridged complexes, on the other hand, a dissymmetric rotation of the C_5 rings is required to avoid an ecliptic conformation at the ethano bridge. The axially symmetric structure of **5**, which arises by dissymmetric rotation of both rings with $\theta \approx +6°$, does indeed generate a staggered conformation at the C–C bridge; it must be unfavorable, however, with regard to intramolecular Cl–H and Cl–C repulsions, since the accessible range of $\theta \approx 6°$, limited by the length of the bridging C–C bond, is far from the energy minimum at $\theta \approx \pm 20°$. The energy changes

(14) For details of this analysis see the Experimental Section.
(15) Included in this potential function are repulsive interactions which depend on θ, i.e. interannular C···C and H···H repulsions.
(16) A slight bending of the C–C bond connecting the bridge with the bridgehead C atoms, out of the plane of the adjacent C_5 ring, is required to accommodate such a distortion. This bending mode is portrayed as very soft by AM1-type model calculations.

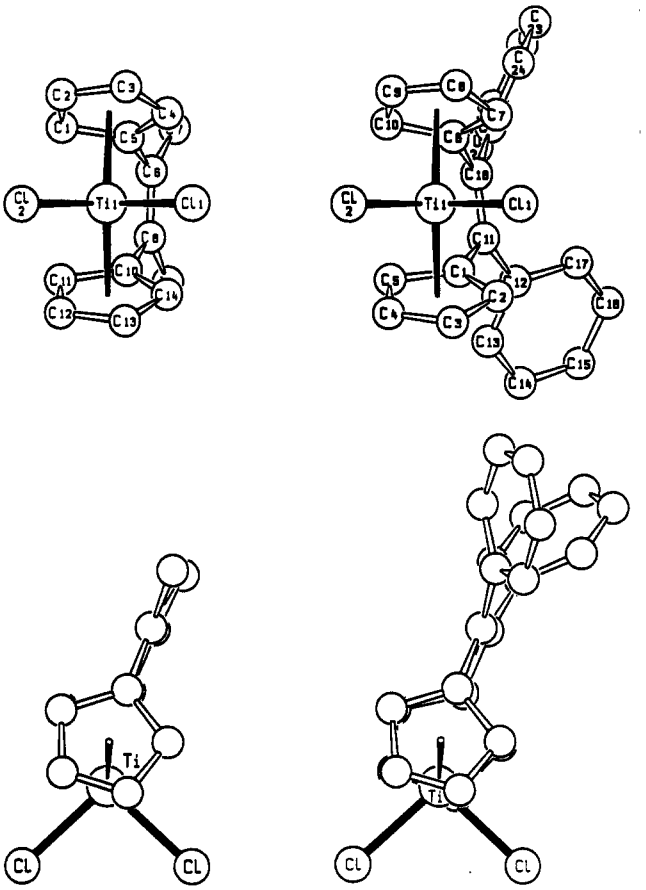

Figure 2. Molecular structures of the etheno-bridged titanocene derivatives $R_2C_2(C_5H_4)_2TiCl_2$: **2** (R = $-CH_3$, left); **3** (R = $-C_6H_5$, right).[11] Projections are parallel to the $TiCl_2$ bisector axis (top) and perpendicular to the $TiCl_2$ plane (bottom).

brought about by an additional consymmetric rotation of the entire ligand framework of such an ethano-bridged metallocene dichloride were studied by subjecting the model complex $(X\text{-}C_5H_4)_2TiCl_2$ with initial, idealized C_2-symmetric geometry, similar to that of complex **5**, to a consymmetric rotation of both C_5 rings with varying angle θ. The resulting energy profile is almost identical with that obtained for the model complex with eclipsed C_5 rings (Figure 6)[17] and indicates that such a molecule should likewise favor a distorted geometry deviating from C_2 symmetry by $\theta \approx 20°$, as observed for complex **4**.

Why then would an *ansa*-metallocene complex such as **5** adopt an axial gometry at all? One factor which might stabilize an axial symmetry is apparent from Figure 7: The crystal structure of **5** contains a number of symmetrically arranged *intermolecular* contacts which tend to hold the $TiCl_2$ group in its place on the molecular and crystallographic C_2 axis, while several nonsymmetric intermolecular contacts apparent in the crystal structure of **4** would seem to reinforce the oblique geometry of this complex molecule.

An additional, probably more important stabilization of axially symmetric geometries is derived from interannular repulsions between those pairs of α-C and α-H atoms which approach each other with increasing consymmetric rotation of the C_5 rings. This effect is particularly pronounced when an additional alkyl (e.g. CH_3) substituent occupies an α-position at each ring ligand. In this case,

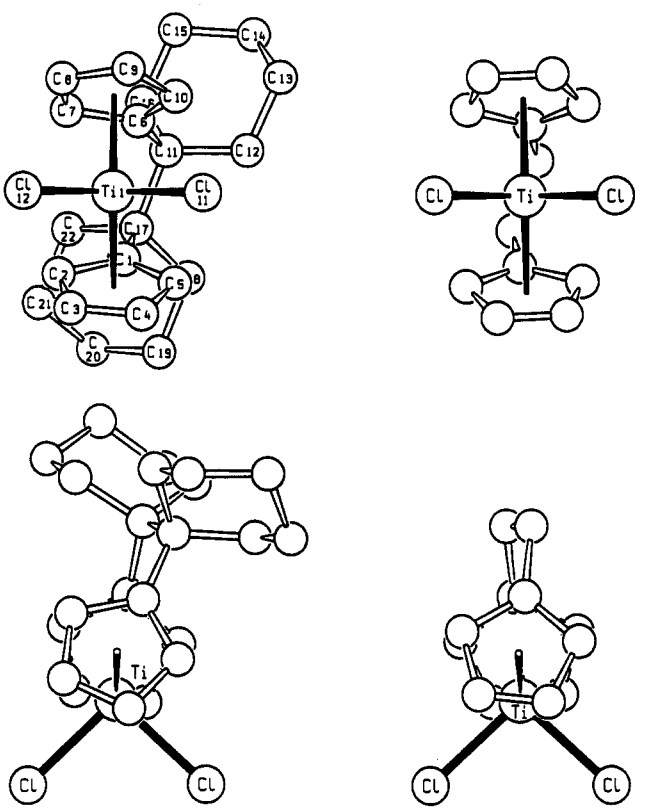

Figure 3. Molecular structures of ethano-bridged titanocene derivatives $R_4C_2(C_5H_4)_2TiCl_2$: **4** (R, R = $-(CH_2)_5-$, left[10]); **5** (R, R = -H, -H, right, as reported in ref 4a). Projections are parallel to the $TiCl_2$ bisector axis (top) and perpendicular to the $TiCl_2$ plane (bottom).

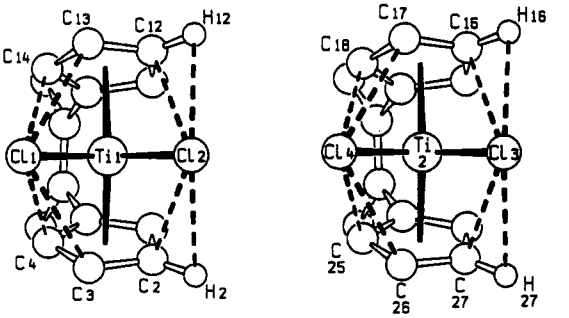

Figure 4. Intramolecular Cl–H and Cl–C contacts (dashed lines) below the van der Waals limit in the crystal structure of **2**.

a relatively steep potential well with a single minimum at $\theta = 0°$ (Figure 6, curve B) is likely to suppress any consymmetric distortions. As these α–α repulsions will be diminished by a dissymetric rotation of the C_5-ring ligands, they would tend to stabilize an axially symmetric *ansa*-metallocene geometry.

Alkyl substituents in a β-position of a C_5 ring, on the other hand, will suffer increased repulsion by the Cl atoms. As a consequence, the energy minima for distorted geometries (Figure 6, curve C) are deepened and shifted to larger values of θ.[18] This effect is the most likely cause for the severe distortions seen in *ansa*-metallocene complexes with bulky alkyl β-substituents of the type represented in Figure 1; here, a consymmetric rotation of the ligand framework

(17) The energy minimum at $\theta \approx 20°$ is slightly deeper for an initial geometry with C_{2v} than with C_2 symmetry. Its depth will depend also on the parametrization of the potential function; a deeper minimum is to be expected, for example, if Coulombic repulsion between negatively charged C and Cl atoms (omitted for simplicity) would be included.

(18) Simulation for idealized C_5 rings carrying a β-carbon atom yields, with otherwise unchanged parameters, an energy minimum of ca. -4 kJ/mol at $\theta \approx 30°$. This result is to be considered as merely suggestive, however, since metal–ring distances vary substantially in heavily substituted *ansa*-metallocenes.[7-9]

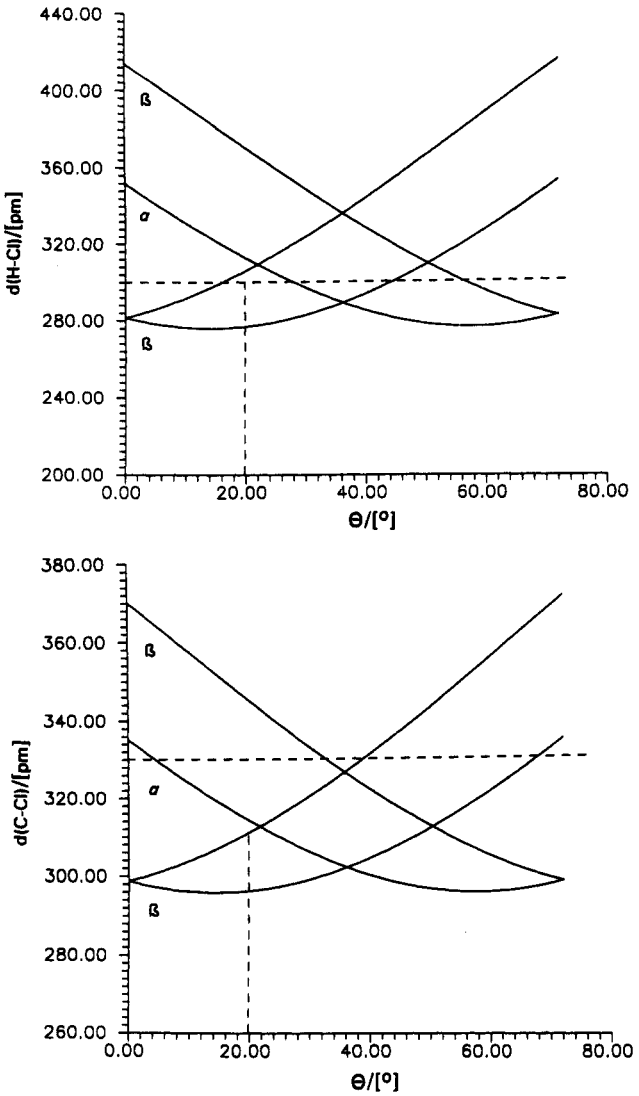

Figure 5. Intramolecular Cl–H and Cl–C contacts for the complex $(X\text{-}C_5H_4)_2TiCl_2$, in dependence on the torsional angle θ by which each C_5 ring is rotated away from an idealized C_{2v}-symmetric geometry. Horizontal dashed lines represent the van der Waals limits; vertical dashed lines at $\theta \approx 20°$ indicate the actual geometry of complexes **2** and **3**.

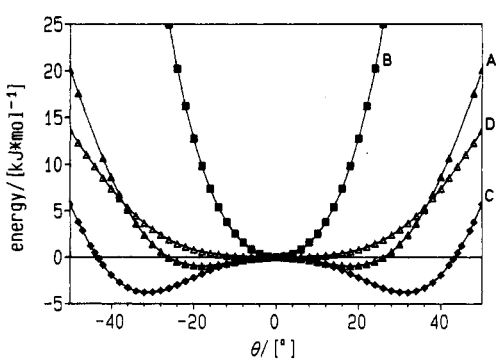

Figure 6. Energy changes caused by consymmetric rotation of both rings with varying torsional angles θ, for a model complex of the type $(X\text{-}C_5H_3R)_2TiCl_2$ (X = void), as obtained by means of a Buckingham-type potential function (see Experimental Section): (A, ▲) unsubstituted (R = H) model for titanocene dichloride with either an etheno or an ethano bridge (initial, idealized geometry of either C_{2v} or C_2 symmetry); (B, ■) C_2-symmetric complex with alkyl substituents in one α-position at each C_5 ring (R_α = C); (C, ◆) analogous complex with alkyl substituents in one β-position of each C_5 ring (R_β = C); (D, △) analogous zirconocene complex $(X\text{-}C_5H_4)_2ZrCl_2$ with increased metal–centroid and metal–Cl distances.

Table IV. Bonding and Nonbonding Distances (in pm) and Bond and Dihedral Angles (in deg) with Esd's in Parentheses for Complex 4, $(C(CH_2)_5)_2[1\text{-}C_5H_4]_2TiCl_2$[a]

	Distances and Angles		
Ti(1)–C(1)	239.0 (4)	Ti(1)–C(6)	239.0 (5)
Ti(1)–C(2)	232.5 (4)	Ti(1)–C(7)	237.1 (5)
Ti(1)–C(3)	237.3 (5)	Ti(1)–C(8)	237.8 (6)
Ti(1)–C(4)	238.1 (6)	Ti(1)–C(9)	235.0 (5)
Ti(1)–C(5)	237.6 (5)	Ti(1)–C(10)	234.1 (5)
Ti(1)–Cl(11)	235.5 (1)	Ti(1)–Cl(12)	235.9 (1)
Cl(11)–Ti(1)–Cl(12)	95.0 (1)		
Ti(1)–CR(1)	204.5	Ti(1)–CR(2)	203.9
CR(1)1–Ti(1)–CR(2)	127.8		
PL(1)–PL(2)	52.1		
C(11)–C(17)	160.2 (6)	C(6)–C(11)–C(17)–C(1)	−29.0 (4)
ZCP(1)–ZZ(1)–ZCL(1)	163.5		
Ti(2)–C(23)	239.8 (5)	Ti(2)–C(28)	238.3 (4)
Ti(2)–C(24)	236.2 (5)	Ti(2)–C(29)	233.6 (4)
Ti(2)–C(25)	239.8 (5)	Ti(2)–C(30)	237.0 (5)
Ti(2)–C(26)	238.5 (4)	Ti(2)–C(31)	240.1 (5)
Ti(2)–C(27)	232.0 (4)	Ti(2)–C(32)	238.0 (4)
Ti(2)–Cl(21)	236.0 (2)	Ti(2)–Cl(22)	235.8 (1)
Cl(21)–Ti(2)–Cl(22)	93.7 (1)		
Ti(2)–CR(3)	204.7	Ti(2)–CR(4)	205.0
CR(3)–Ti(2)–CR(4)	127.6		
PL(3)–PL(4)	53.4		
C(33)–C(39)	160.9 (5)	C(28)–C(33)–C(39)–C(23)	−31.9 (4)
ZCP(2)–ZZ(2)–ZCL(2)	161.5		
	Intramolecular Contacts		
Cl(11)···H(4)	290	Cl(11)···H(10)	298
Cl(12)···H(3)	282	Cl(12)···H(8)	281
Cl(12)···C(3)	298	Cl(12)···C(8)	297
Cl(21)···H(26)	287	Cl(21)···H(31)	289
Cl(22)···H(25)	292	Cl(22)···H(29)	295

[a] Legend: CR = centroid; PL = mean plane of η^5-C_5 ring; ZCP = midpoint of the vector connecting the two bridgehead carbon atoms C(1), C(6) and C(23), C(28); ZCL = midpoint of the Cl–Cl vector; ZZ = midpoint of the CR–CR vector.

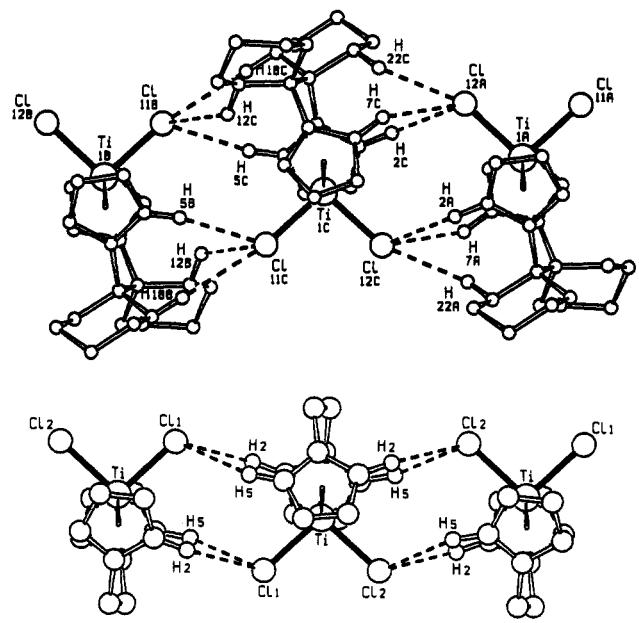

Figure 7. *Intermolecular* Cl–H contacts below 2.9 Å in the crystal structures of complex **4** (top) and complex **5** (bottom[4a]).

by $\theta \approx 36°$ is indeed observed in the crystalline state.

In $CDCl_3$ or C_6D_6 solution, however, all of the *ansa*-metallocene complexes considered give rise to ^1H and ^{13}C NMR spectra which correspond to an axially symmetric molecular structure.[8,10,11] Even in the case of the severely distorted complex **1**, no coalescence is observed down to temperatures of ca. −80 °C. In solution, these complexes

Table V. Crystallographic and Experimental Data for $C_2(CH_3)_4[1\text{-}C_5H_3\text{-}3\text{-}C(CH_3)_2(2'\text{-}C_4H_3O)]_2TiCl_2$ (1), $C_2(CH_3)_2[1\text{-}C_5H_4]_2TiCl_2$ (2), $C_2(C_6H_5)_2[1\text{-}C_5H_4]_2TiCl_2$ (3), and $(C(CH_2)_5)_2[1\text{-}C_5H_4]_2TiCl_2$ (4)[a]

	1	2	3	4
formula	$C_{30}H_{36}O_2TiCl_2$	$C_{14}H_{14}TiCl_2$	$C_{24}H_{18}TiCl_2$	$C_{22}H_{28}TiCl_2$
fw	547.4	301.1	425.2	411.3
cryst color, form	red cube	red parallelepiped	red cube	red cube
cryst syst	monoclinic	orthorhombic	monoclinic	triclinic
space group	$P2_1/c$ (No. 14)	$P2_12_12_1$ (No. 19)	$P2_1/c$ (No. 14)	$P\bar{1}$ (No. 2)
a, pm	959.4 (3)	771.9 (1)	864.7	1072.8 (2)
b, pm	1284.2 (3)	1785.3 (4)	1611.3 (7)	1266.0 (3)
c, pm	2379.9 (7)	1883.6 (3)	1377.6 (7)	1511.0 (3)
α, deg				80.66 (3)
β, deg	111.73 (2)		91.48 (4)	89.04 (3)
γ, deg				76.20 (3)
V, 10^6 pm^3	2723.6 (13)	2596 (1)	1918.8 (15)	1966.1 (7)
d_{calcd}, g/cm^3	1.33	1.54	1.47	1.39
Z	4	8	4	4
cryst dimens, mm	0.3 × 0.3 × 0.3	0.5 × 0.4 × 0.5	0.2 × 0.2 × 0.2	0.2 × 0.2 × 0.2
abs coeff (μ), cm^{-1}	5.3	10.4	7.3	7.1
T, K	223	239	233	233
weighting scheme	$w^{-1} = \sigma^2(F) + 0.0008F^2$	unit weight	$w^{-1} = \sigma^2(F) + 0.0004F^2$	$w^{-1} = \sigma^2(F) + 0.0008F^2$
scan mode	Wyckoff ω scan	Wyckoff ω scan	Wyckoff ω scan	Wyckoff ω scan
scan range, deg	0.7	1.0	0.8	0.7
2θ limits, deg	$4.0 \le 2\theta \le 52.0$	$4.0 \le 2\theta \le 52.0$	$4.0 \le 2\theta \le 54.0$	$4.0 \le 2\theta \le 52.0$
scan speed, deg/min	2.0–29.3	2.4–29.3	2.0–29.3	2.0–29.3
no. of data collected	5191	2927	2470	5881
no. of unique data	3434	2733	1428	4311
observn criterion	$I \ge 3.0\sigma(I)$	$I \ge 1.5\sigma(I)$	$I \ge 3.0\sigma(I)$	$I \ge 3.0\sigma(I)$
no. of params	317	319	124	411
R_F[b]	0.055	0.033	0.085	0.047
R_{wF}[c]	0.066	0.036	0.098	0.060
residual density, 10^{-6} e pm^{-3}	1.08	0.3	0.62	0.39

[a] Conditions: Syntex/Siemens-P3 four-cycle diffractometer, Mo Kα radiation, graphite monochromator. [b] $R_F = \sum||F_o| - |F_c||/\sum|F_o\delta|$. [c] $R_{wF} = [\sum w(|F_o| - |F_c|)^2/\sum F_o^2]^{1/2}$, with $w = [\sigma^2(F)]^{-1}$.

thus appear to undergo an unrestricted fluctuation between their two unsymmetrically distorted geometries. From the shallow energy threshold apparent in Figure 6 at $\theta = 0°$ one would indeed expect a very low activation energy for this fluctuation. Species of this type, rather than being stereorigid, thus have their ligand framework freely librating relative to the $TiCl_2$ unit with angular amplitudes of up to 70–80°.

With regard to the influence of different interannular bridges on the stereoridigity of *ansa*-metallocenes, it has been noted that longer bridges with more than two C or Si atoms will invariably lead to an unsymmetrically distorted metallocene geometry to accommodate the increased distances between the bridgehead atoms.[6,19-21] For monosilano-bridged complexes, on the other hand, the very short distance between both bridgehead atoms would lead one to expect a strict adherence to a C_2-symmetric geometry. While an axially symmetric structure has indeed been found for the dimethylsilano-bridged titanocene complex $(CH_3)_2Si(C_5H_4)_2TiCl_2$ (**6**),[22,23a] an off-axial distortion with $\theta \approx \pm 20°$, almost identical with that discussed above for complexes **2** and **3**, has been reported by Petersen and co-workers[23b] for the corresponding dimethylsilametallacyclobutane derivative $(CH_3)_2Si(C_5H_4)_2Ti(CH_2)_2Si(CH_3)_2$ (**7**; Figure 8). As we cannot discern any intermolecular contacts in the crystal structure of **7**, we have to assume again that intramolecular repulsion of β-H and -C atoms of the ring ligands, in this case by the methylene H atoms

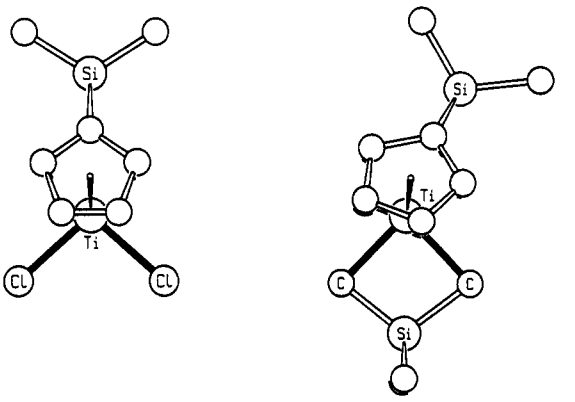

Figure 8. Molecular structures reported in ref 22 and 23a for dimethylsilano-bridged titanocene complexes: $(CH_3)_2Si(C_5H_4)_2TiCl_2$ (**6**, left) and $(CH_3)_2Si(C_5H_4)_2Ti(CH_2)_2Si(CH_3)_2$ (**7**, right). Projections are perpendicular to the $TiCl_2$ plane (**6**) and to the TiC_2 plane (**7**).

of the silacyclobutane ring, cause the distortion of this silano-bridged metallocene complex. This example illustrates the influence of different coligands on the balance between axial and distorted *ansa*-metallocene geometries.

Finally, preferred conformations of the homologous *ansa*-zirconocene complexes were studied by application of the rotational potential function described above to the model species $(X\text{-}C_5H_4)_2ZrCl$ with typical zirconium–centroid and zirconium–chloride distances of 210 and 245 pm. Here, we find a single energy minimum at $\theta = 0°$, since all intramolecular repulsions are now reduced in weight (Figure 6, curve D). The resulting energy profile is quite unusually shallow, however, up to values of $\theta \approx \pm 30°$. It will probably be further flattened out whenever alkyl substituents occupy a β-position at each ring. Chiral *ansa*-zirconocene complexes—rather than being stereorigid as hitherto assumed—thus appear just as prone to undergo thermally induced excursions of ±20–40° from the pri-

(19) (a) Davis, B. R.; Bernal, I. *J. Organomet. Chem.* **1971**, *30*, 75. (b) Epstein, E. F.; Bernal, I. *Inorg. Chim. Acta* **1973**, *7*, 211.
(20) Curtis, M. D.; D'Errico, J. J.; Duffy, D. N.; Epstein, P. S.; Bell, L. G. *Organometallics* **1983**, *2*, 1808.
(21) Röll, W.; Zsolnai, L.; Huttner, G.; Brintzinger, H. H. *J. Organomet. Chem.* **1987**, *322*, 65.
(22) Köpf, H.; Pickardt, J. *Z. Naturforsch., B* **1981**, *36*, 1208.
(23) (a) Bajgur, C. S.; Tikkanen, W. R.; Petersen, J. L. *Inorg. Chem.* **1985**, *24*, 2539. (b) Kabi-Satpathy, A.; Bajgur, C. S.; Reddy, K. P.; Petersen, J. L. *J. Organomet. Chem.* **1989**, *364*, 105.

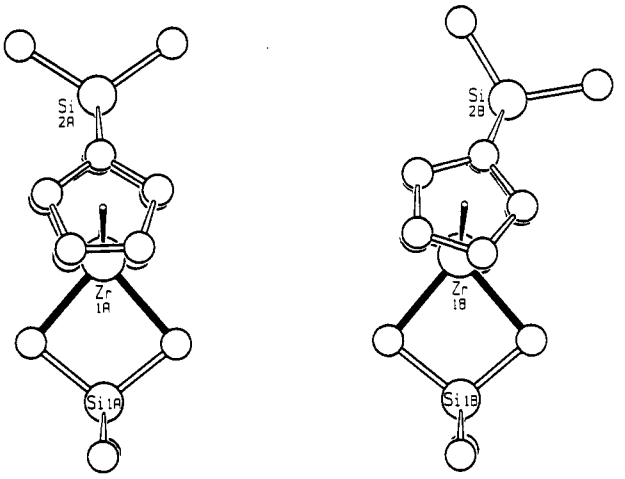

Figure 9. Molecular structures reported by Petersen and co-workers[23b] for two crystallographically independent molecules of $(CH_3)_2Si(C_5H_4)_2Zr(CH_2)_2Si(CH_3)_2$ (8). Projections are perpendicular to the ZrC_2 plane.

marily expected axially symmetric geometry as their titanium analogues.

An interesting case in point is the zirconium analogue 8 of the dimethylsilyl-bridged complex 7. For this compound, Petersen and co-workers have reported a crystal structure which contains, in addition to an axially symmetric molecule (**8A**), a second molecule (**8B**) with distorted geometry; the latter deviates from C_2-axial symmetry again by $\theta \approx 20°$ (Figure 9).[23b] As predicted from Figure 5, one observes a closer contact between the methylene H atoms of the midplane ligand and the β-C atoms of the C_5 rings (2.88 Å) in the undistorted than in the distorted molecule (2.98 and 3.11 Å). In addition, a weak intermolecular contact (2.99 Å) between an H atom at the dimethylsilyl bridge and a C_5-ring C atom of an adjacent A-type molecule appears to stabilize the distorted geometry of **8B**, like those of complexes **3** and **4** discussed above. This case nicely illustrates the near-equal stabilities of axially symmetric and distorted geometries of *ansa*-zirconocene complexes.

The notion that *ansa*-metallocene complexes are fairly easily deformable—to a degree which will depend on their substitution patterns—must obviously have implications for structure–function correlations in homogeneous Ziegler–Natta catalysis. An increase in stereoselectivity which is brought about by the introduction of α-methyl substituents in chiral *ansa*-metallocene catalysts,[24,25] for example, is most likely connected to a decreased tendency of these α-substituted complexes to undergo thermally induced excursions from axial symmetry (cf. Figure 6). It remains to be clarified if and in which way other properties of these catalysts are related to the ease with which these complex molecules can deviate from axial symmetry.

Experimental Section

Crystal and Molecular Structures of Complexes 1–4. Suitable crystals for X-ray crystal structure determinations were obtained by slow evaporation of diethyl ether solutions of the *ansa*-titanocene dichlorides 1–4. The crystals were sealed in thin-walled capillaries, transferred to a Syntex/Siemens-P3 four-circle diffractometer equipped with a graphite monochromator (Mo Kα radiation, λ = 71.073 pm), and cooled to the temperature referred to in Table V. Final unit-cell parameters for complex 1–4 were obtained by least-squares analysis of 24 well-centered reflections. During data collection the intensities of 3 standard reflections were measured every 100 reflections. These showed no significant variation for complexes **1**, **2**, and **4**, while significant decay of the intensities of the standard reflections was observed for complex **3** during measurement (vide infra). The data were scaled by the standard reflections and corrected for Lorentz and polarization effects. The crystallographic and experimental data for complexes 1–4 are summarized in Table V.

For solution and refinement the data were used without absorption correction. The structures of **1–4** were solved by direct methods (**1–3**, SHELXTL PLUS; **4**, SHELXS86) and refined by full-matrix least-squares techniques (**1–3**, SHELXTL PLUS; **4**, SHELX76), minimizing the function $\sum w(|F_o| - |F_c|)^2$, where w was calculated from $w = [\sigma^2(F)]^{-1}$. The hydrogen atoms were calculated in idealized positions and included in the refinement by applying a riding model.

For refinement of the crystal structures of the *ansa*-titanocene dichlorides **1** and **2**, an anisotropic model was applied, giving final R values of 0.055 (R_F) and 0.066 (R_{wF}) for complex **1** and of 0.033 and 0.036 (R_F, R_{wF}) for titanium complex **2**; the latter crystallized with two independent molecules with almost identical bonding features in the unit cell. Structural parameters of **1** and **2** are presented in Tables I and II.

During measurement of *ansa*-titanocene complex **3**, degradation of the crystal was observed by a significant decrease of the check reflection intensities,[26] thus limiting the reflection array to 1428 independent intensities with $I \geq 3\sigma(I)$. A partially anisotropic model was used for refinement (carbon atoms were refined isotropically), which converged at final R values of R_F = 0.085 and

Table VI. Fractional Coordinates (×10⁴) (with Esd's) and Isotropic Parameters (pm² × 10⁻¹) for Complex 1, *rac*-$C_2(CH_3)_4[1\text{-}C_5H_3\text{-}3\text{-}C(CH_3)_2(2'\text{-}C_4H_3O)]_2TiCl_2$

atom	x	y	z	U^a
Ti(1)	4235 (1)	5183 (1)	2543 (1)	18 (1)
Cl(1)	6505 (1)	4789 (1)	2448 (1)	29 (1)
Cl(2)	3913 (1)	3518 (1)	2921 (1)	31 (1)
C(1)	3347 (5)	6343 (3)	3084 (2)	21 (1)
C(2)	4248 (5)	5644 (3)	3526 (2)	24 (2)
C(3)	5772 (5)	5755 (3)	3599 (2)	22 (2)
C(4)	5810 (5)	6539 (3)	3182 (2)	24 (2)
C(5)	4364 (5)	6908 (3)	2877 (2)	20 (1)
C(6)	7130 (5)	5278 (4)	4103 (2)	29 (2)
C(7)	6928 (7)	4103 (4)	4184 (2)	47 (2)
C(8)	8577 (6)	5457 (5)	3989 (2)	53 (2)
C(9)	7225 (5)	5836 (3)	4671 (2)	31 (2)
C(10)	7570 (8)	7198 (5)	5258 (2)	65 (3)
C(11)	7215 (7)	6454 (5)	5545 (2)	59 (3)
C(12)	6968 (6)	5565 (4)	5172 (2)	46 (2)
C(13)	1663 (5)	6485 (3)	2887 (2)	24 (2)
C(14)	1002 (5)	5577 (4)	3121 (2)	37 (2)
C(15)	1355 (6)	7494 (4)	3171 (2)	41 (2)
C(16)	944 (5)	6538 (3)	2160 (2)	22 (1)
C(17)	953 (5)	7649 (3)	1920 (2)	32 (2)
C(18)	−703 (5)	6183 (4)	1909 (2)	35 (2)
C(19)	1859 (5)	5820 (3)	1914 (2)	21 (1)
C(20)	2888 (5)	6128 (3)	1645 (2)	21 (1)
C(21)	3383 (5)	5246 (3)	1413 (2)	22 (1)
C(22)	2755 (5)	4371 (3)	1591 (2)	22 (1)
C(23)	1801 (5)	4723 (3)	1883 (2)	23 (1)
C(24)	4167 (5)	5273 (3)	959 (2)	24 (1)
C(25)	5331 (5)	6144 (4)	1098 (2)	35 (2)
C(26)	4883 (6)	4217 (4)	917 (2)	38 (2)
C(27)	2920 (5)	5516 (3)	365 (2)	28 (2)
C(28)	908 (8)	5120 (7)	−416 (3)	87 (3)
C(29)	1181 (7)	6090 (6)	−480 (3)	64 (3)
C(30)	2434 (7)	6370 (5)	54 (3)	81 (3)
O(1)	7568 (5)	6854 (3)	4705 (2)	65 (2)
O(2)	1967 (5)	4704 (3)	99 (2)	70 (2)

[a] Equivalent isotropic U defined as one-third of the orthogonalized U_{ij} tensor.

(24) Miya, S.; Yoshimura, T.; Mise, T.; Yamazaki, H. *Polymer Prepr. Jpn.* **1988**, *37*, 285. Mise, T.; Miya, S.; Yamazaki, H. *Chem. Lett.* **1989**, 1853.

(25) Röll, W.; Brintzinger, H. H.; Rieger, B.; Zolk, R. *Angew. Chem.* **1990**, *102*, 339.

(26) The final intensities of the standard reflections were approximately 60% of those at the beginning.

Table VII. Fractional Coordinates (×10⁴) (with ESD's) and Isotropic Parameters (pm² × 10⁻¹) for Complex 2, $C_2(CH_3)_2[1\text{-}C_5H_4]_2TiCl_2$

atom	x	y	z	U[a]
Ti(1)	1258 (1)	5969 (1)	629 (1)	19 (1)
Cl(1)	1105 (2)	7275 (1)	832 (1)	36 (1)
Cl(2)	3 (2)	5626 (1)	1719 (1)	35 (1)
C(1)	-148 (6)	5097 (3)	-116 (2)	29 (1)
C(2)	-1469 (6)	5474 (3)	245 (3)	35 (1)
C(3)	-1431 (6)	6233 (3)	55 (2)	34 (1)
C(4)	-91 (6)	6322 (2)	-450 (2)	27 (1)
C(5)	694 (5)	5625 (2)	-569 (2)	24 (1)
C(6)	2197 (6)	5469 (2)	-1039 (2)	27 (1)
C(7)	1844 (7)	5360 (3)	-1818 (2)	36 (1)
C(8)	3745 (6)	5430 (2)	-739 (2)	26 (1)
C(9)	5434 (6)	5249 (3)	-1098 (3)	38 (2)
C(10)	3819 (5)	5572 (3)	41 (2)	26 (1)
C(11)	3445 (6)	5047 (3)	587 (2)	33 (1)
C(12)	3665 (7)	5411 (3)	1245 (2)	40 (2)
C(13)	4086 (6)	6161 (3)	1121 (2)	38 (2)
C(14)	4188 (5)	6270 (3)	371 (2)	31 (1)
Ti(2)	7544 (1)	2913 (1)	1332 (1)	21 (1)
Cl(3)	10507 (1)	3227 (1)	1262 (1)	41 (1)
Cl(4)	6825 (2)	3541 (1)	271 (1)	30 (1)
C(15)	7776 (6)	1672 (2)	1723 (3)	31 (1)
C(16)	8822 (7)	1715 (3)	1104 (3)	36 (1)
C(17)	7771 (6)	1874 (2)	526 (3)	32 (1)
C(18)	6026 (6)	1909 (2)	766 (2)	30 (1)
C(19)	6022 (6)	1776 (2)	1511 (2)	25 (1)
C(20)	4492 (6)	1774 (3)	1983 (2)	28 (1)
C(21)	3315 (7)	1098 (3)	1958 (3)	43 (2)
C(22)	4228 (5)	2379 (2)	2380 (2)	26 (1)
C(23)	2780 (7)	2498 (3)	2902 (3)	38 (2)
C(24)	5460 (6)	3013 (2)	2265 (2)	25 (1)
C(25)	5199 (6)	3612 (2)	1791 (2)	28 (1)
C(26)	6653 (7)	4094 (3)	1816 (2)	34 (1)
C(27)	7818 (7)	3791 (3)	2302 (2)	36 (1)
C(28)	7133 (6)	3120 (3)	2569 (2)	34 (1)

[a] Equivalent isotropic U defined as one-third of the orthogonalized U_{ij} tensor.

Table VIII. Fractional Coordinates (×10⁴) (with Esd's) and Isotropic Parameters (pm² × 10⁻¹) for Complex 3, $C_2(C_6H_5)_2[1\text{-}C_5H_4]_2TiCl_2$

atom	x	y	z	U[a]
Ti(1)	7740 (4)	6949 (1)	-176 (1)	33 (1)
Cl(1)	6351 (6)	8122 (2)	269 (2)	57 (2)
Cl(2)	7350 (6)	7144 (2)	-1851 (2)	49 (2)
C(1)	7336 (19)	5805 (6)	866 (7)	25 (3)
C(2)	6076 (20)	6316 (7)	956 (8)	34 (3)
C(3)	5220 (22)	6319 (7)	15 (8)	42 (3)
C(4)	6033 (20)	5812 (7)	-594 (8)	35 (3)
C(5)	7392 (19)	5505 (6)	-107 (7)	31 (3)
C(6)	10034 (21)	6654 (7)	789 (8)	35 (3)
C(7)	9601 (19)	7492 (7)	909 (8)	34 (3)
C(8)	9843 (24)	7897 (9)	27 (10)	60 (4)
C(9)	10313 (22)	7334 (8)	-646 (9)	56 (4)
C(10)	10442 (22)	6526 (8)	-209 (9)	48 (4)
C(11)	8559 (19)	5630 (6)	1652 (6)	21 (2)
C(12)	8116 (19)	5066 (6)	2451 (7)	22 (2)
C(13)	7296 (19)	4351 (7)	2274 (8)	34 (3)
C(14)	6811 (22)	3858 (8)	3044 (8)	47 (4)
C(15)	7128 (20)	4076 (8)	3967 (8)	43 (3)
C(16)	7962 (21)	4803 (7)	4170 (8)	39 (3)
C(17)	8421 (20)	5314 (8)	3408 (8)	39 (3)
C(18)	9855 (20)	6002 (6)	1556 (7)	23 (3)
C(19)	11348 (20)	5880 (6)	2165 (7)	24 (3)
C(20)	11768 (20)	5105 (7)	2515 (7)	32 (3)
C(21)	13079 (20)	5001 (7)	3126 (8)	41 (3)
C(22)	13986 (21)	5678 (7)	3377 (8)	40 (3)
C(23)	13656 (22)	6441 (7)	3033 (8)	40 (3)
C(24)	12333 (20)	6547 (7)	2431 (7)	34 (3)

[a] Equivalent isotropic U defined as one-third of the orthogonalized U_{ij} tensor.

R_{wF} = 0.098 with a residual electron density of 0.62 × 10⁻⁶ e pm⁻³. Structural parameters of complex 3 are presented in Table III.

Table IX. Fractional Coordinates (×10⁴) (with Esd's) and Isotropic Parameters (pm² × 10⁻¹) for Complex 4, $(C(CH_2)_5)_2[1\text{-}C_5H_4]_2TiCl_2$

atom	x	y	z	U[a]
Ti(1)	302 (1)	7548 (1)	5348 (1)	27 (1)
Cl(11)	41 (2)	5988 (1)	6347 (1)	49 (1)
Cl(12)	-486 (1)	8807 (1)	6335 (1)	39 (1)
C(1)	-167 (4)	7699 (3)	3785 (2)	25 (2)
C(2)	-806 (5)	8687 (3)	4103 (3)	31 (2)
C(3)	-1750 (5)	8458 (4)	4699 (3)	43 (2)
C(4)	-1677 (6)	7334 (4)	4802 (3)	43 (2)
C(5)	-711 (5)	6857 (3)	4257 (3)	34 (2)
C(6)	2208 (5)	7199 (3)	4493 (2)	28 (2)
C(7)	2035 (5)	8264 (3)	4729 (3)	29 (2)
C(8)	2158 (5)	8149 (4)	5671 (3)	40 (2)
C(9)	2355 (5)	7043 (4)	6033 (3)	46 (2)
C(10)	2385 (5)	6447 (3)	5310 (3)	38 (2)
C(11)	2207 (5)	6939 (3)	3541 (2)	26 (2)
C(12)	2469 (5)	5672 (3)	3572 (3)	34 (2)
C(13)	3821 (5)	5011 (3)	3888 (3)	38 (2)
C(14)	4833 (5)	5459 (4)	3350 (3)	48 (2)
C(15)	4645 (5)	6673 (4)	3406 (3)	46 (2)
C(16)	3338 (5)	7332 (3)	3041 (3)	32 (2)
C(17)	850 (5)	7573 (3)	3067 (2)	25 (2)
C(18)	420 (5)	6935 (3)	2379 (2)	35 (2)
C(19)	-836 (5)	7552 (4)	1886 (3)	42 (2)
C(20)	-728 (6)	8663 (4)	1367 (3)	48 (2)
C(21)	-340 (5)	9348 (3)	2017 (3)	37 (2)
C(22)	889 (5)	8729 (3)	2538 (3)	33 (2)
Ti(2)	4422 (1)	7450 (1)	9845 (1)	28 (1)
Cl(21)	3453 (1)	6165 (1)	10729 (1)	43 (1)
Cl(22)	3130 (1)	8973 (1)	10402 (1)	47 (1)
C(23)	6643 (5)	7400 (3)	9574 (2)	25 (1)*
C(24)	6157 (5)	8211 (3)	10121 (2)	32 (2)
C(25)	5843 (5)	7703 (3)	10959 (3)	37 (2)
C(26)	6071 (5)	6571 (3)	10945 (3)	39 (2)
C(27)	6506 (5)	6382 (3)	10083 (3)	31 (2)
C(28)	4826 (5)	7874 (3)	8287 (2)	25 (2)
C(29)	3636 (5)	8548 (4)	8482 (3)	38 (1)*
C(30)	2757 (5)	7879 (4)	8740 (3)	44 (2)
C(31)	3398 (5)	6803 (4)	8710 (3)	40 (2)
C(32)	4665 (5)	6774 (3)	8456 (3)	32 (1)*
C(33)	6024 (5)	8228 (3)	7949 (2)	21 (1)*
C(34)	6306 (5)	7923 (3)	6998 (2)	33 (2)
C(35)	5281 (5)	8601 (4)	6290 (3)	43 (2)
C(36)	5220 (6)	9825 (4)	6215 (3)	47 (2)
C(37)	4857 (5)	10183 (3)	7117 (3)	41 (2)
C(38)	5830 (5)	9497 (3)	7860 (3)	32 (2)
C(39)	7184 (4)	7581 (3)	8641 (2)	24 (1)*
C(40)	8194 (5)	8253 (3)	8676 (3)	29 (1)*
C(41)	9355 (5)	7635 (3)	9282 (3)	41 (1)*
C(42)	10036 (5)	6569 (4)	8956 (3)	42 (2)
C(43)	9099 (5)	5854 (3)	8941 (3)	39 (2)
C(44)	7897 (5)	6461 (3)	8370 (3)	30 (1)*

[a] Equivalent isotropic U defined as one-third of the orthogonalized U_{ij} tensor. Asterisks denote isotropically refined C atoms.

Two independent molecules which are almost identical in their essential bonding features are found in the crystal structure of 4. Refinement using a partially anisotropic model[27] converged at final R values of R_F = 0.047 and R_{wF} = 0.060 with a residual electron density of 0.39 × 10⁻⁶ e pm⁻³. Structural parameters of 4 are presented in Table IV.

Further details of these crystal structure determinations are available from Fachinformationszentrum Karlsruhe, D-7514 Eggenstein-Leopoldshafen 2, FRG, by quotation of deposit number CSD-55560, the authors, and the journal reference of this article.

Conformational Analysis. The conformational analysis of the metallocene considered was conducted in the following manner: As a starting geometry we constructed an idealized $[X\text{-}C_5H_4]_2TiCl_2$ molecule in a C_{2v}-symmetric conformation, using cyclopentadienyl ligands with local D_{5h} symmetry ($d_{C\text{-}C}$ = 139 pm, $d_{C\text{-}H}$ = 108 pm),[28] with centroid–metal and Cl–metal distances

(27) The number of reflection data (4311) was insufficient for a completely anisotropic refinement.

of 206 and 235 pm and centroid–metal–centroid and Cl–metal–Cl angles of 128 and 95°, respectively, taken from the average of the crystal structures of **2** and **3**. The two ring-C atoms C_X farthest from the Cl ligands were positioned in the mirror plane which bisects the $TiCl_2$ angle.

This model was subjected to a consymmetric rotation of both C_5 rings about the respective metal–centroid axis with increasing rotational angle θ, defined as the deviation of the vector from the metal to the midpoint of the two C_X atoms from the $TiCl_2$ bisector axis. Cl–C and Cl–H distances determined for rotational angles $0 < \theta < 72°$ are represented in Figure 5. The close coincidence of the Cl–C and Cl–H distances calculated for $\theta \simeq 20°$ with those observed in the crystal structures of complexes **2** and **3** (see Figure 2) documents the validity of our geometrical model.

A similar analysis was conducted for ethano-bridged titanocene complexes. Starting with an analogous $[X\text{-}C_5H_4]_2TiCl_2$ model of C_2 symmetry, in which the two rings are rotated relative to the $TiCl_2$ bisector axis in a dissymmetric manner by 6° (i.e. relative to each other by an angle of 12°, as observed in the C_2-symmetric structure of **5**), consymmetric rotation of both rings was modeled for varying angles θ, as defined above. The resulting variation of Cl–C and Cl–H distances with θ was found to be quite similar to that shown in Figure 5; the experimental data for complex **4** agree, again, with those expected for a consymmetric rotation with $\theta \simeq 20°$.

Relative energies in dependence on the rotational angle θ were estimated by use of a van der Waals potential function of the type $V = A \exp(-Br) - Cr^{-6}$.[29] This Buckingham-type potential is contained in the modeling program MOLDRAW.[31] When applied to a consymmetric rotation of the ligand framework of the model complex $[X\text{-}C_5H_4]_2TiCl_2$, with X = H and an initial geometry of idealized C_{2v} symmetry, this potential function leads to an energy minimum at $\theta = 36°$, due to the repulsion of the two H_X atoms which appears to outweigh all other repulsive interactions. The situation in an *ansa*-metallocene complex was then modeled by deleting these two H_X atoms. The resulting energy profile for consymmetric ligand rotation is shown in Figure 6; the minimum at $\theta \simeq 20°$ reproduces exactly the geometry observed for complexes **2** and **3**. A practically identical energy profile, with energy minima at $\theta \simeq 20°$, is obtained for the C_2-symmetric complex with dissymmetrically staggered C_5 rings, discussed above as a model for ethano-bridged *ansa*-metallocene complexes such as **4**.

ansa-Titanocene complexes with alkyl substituents, either in α or in β positions, were modeled by replacing, in the C_2-symmetric model for ethano-bridged metallocene complexes, the respective H atom at each C_5 ring by a C atom ($d_{C\text{-}C}$ = 150 pm), so as to generate the axially symmetric species $[X\text{-}C_5H_3C]_2TiCl_2$. The potential energy changes associated with consymmetric rotation of these substituted rings are likewise shown in Figure 6 (curves B and C, respectively).

The analogous complex $[X\text{-}C_5H_4]_2ZrCl_2$ was modeled by adjusting the centroid–metal and Cl–metal distances to values of 210 and 245 pm and the centroid–metal–centroid and Cl–metal–Cl angles to values of 125 and 100°, respectively.[7] The resulting energy profile is also represented in Figure 6 (curve D).

Acknowledgment. We thank Mr. M.-H. Prosenc and Professor J. L. Petersen for helpful comments. Financial support of this work by the VW Stiftung, by the Fonds der Chemischen Industrie, and by funds from the University of Konstanz is gratefully acknowledged.

Supplementary Material Available: Listings of crystal data, data collection, and solution and refinement details of the X-ray diffraction studies, bond distances and angles, anisotropic displacement coefficients, and hydrogen atom positional parameters and isotropic displacement coefficients for complexes **1–4** (23 pages); listings of observed and calculated structure factors (55 pages). Ordering information is given on any current masthead page.

(28) The C–H bond distance used (108 pm) is the mean values of the cyclopentadienyl C–H bond lengths determined for $(CH_2)_3(C_5H_4)TiCl_2$ by neutron diffraction.[19b]

(29) A similar approach has been described for the conformational analysis of a monocylcopentadienyliron complex by Coville and coworkers.[30] These authors used an additional torsional potential for the rotation of the cyclopentadienyl ring relative to the $Fe(CO)I(PR_3)$ fragment.

(30) Du Plooy, K. E.; Marais, C. F.; Carlton, L.; Hunter, R.; Boeyens, J. C. A.; Coville, N. J. *Inorg. Chem.* **1989**, *28*, 3855.

(31) Program MOLDRAW; Dipartimento di Chimica-Fisica, Universita di Torino Via P. Guria 7, I-10125 Torino, Italy, 1988. The parameters *A*, *B*, and *C* for C, H, and Cl atoms, included in this program, were used without change. As metal–carbon, metal–hydrogen, and metal–chlorine distances are left unchanged by rotation of the C_5 rings, metal atoms were omitted from the Buckingham potential function.